JOURNAL OF APPLIED PHYSICS VOLUME 94, NUMBER 5 1 SEPTEMBER 2003

Simulation of a two-dimensional sheath over a flat wall with an insulator/conductor interface exposed to a high density plasma

Doosik Kim and Demetre J. Economou[a)]
Plasma Processing Laboratory, Department of Chemical Engineering, University of Houston, Houston, Texas 77204-4004

(Received 28 March 2003; accepted 16 June 2003)

The structure of the two-dimensional (2D) sheath over a flat, electrically inhomogeneous wall exposed to a high density plasma was investigated by a fluid model. The wall consisted of a floating semi-infinite insulator in contact with a semi-infinite conductor biased by a negative dc voltage. The difference in sheath potential over the two materials resulted in a 2D sheath over the insulator/conductor interface. The ion flux was higher on the conductor side of the interface at the expense of the flux on the insulator side. The spatial extend and magnitude of the ion flux disturbance scaled with the difference in the sheath thickness over the two different materials. The ion impact angle along the surface increased progressively as the material interface was approached. Sheath distortion was exacerbated when the electron temperature was decreased or the bias potential was made more negative. © *2003 American Institute of Physics.* [DOI: 10.1063/1.1597943]

I. INTRODUCTION

A sheath forms over any surface in contact with plasma. The sheath over a flat, infinite, homogeneous surface is one dimensional (1D), with the sheath electric field pointing perpendicular to the surface. When the surface contains topographical features, however, the sheath is no longer one dimensional. The extend of sheath "disturbance" depends on the thickness of the sheath compared to the size of the topographical features. When the sheath thickness is comparable to or smaller than the length scale of the surface features, the sheath tends to wrap around the contour of the features. This is called plasma molding.[1–3]

A multidimensional sheath can also arise over a perfectly flat surface, when this surface is electrically inhomogeneous. Consider, for example, the situation depicted in Fig. 1. A flat, electrically inhomogeneous wall is exposed to a high density plasma. The conductor side of the material interface is biased by a negative dc potential, while the insulator side is electrically floating. Upon exposure to plasma, the insulator will charge up to reach the floating potential, while the conductor potential can be varied at will. For given plasma density and electron temperature (e.g., given Debye length), the difference in sheath potentials over the two sides of the interface will result in different sheath thicknesses. A schematic of the plasma/sheath interface is also shown in Fig. 1. When the dc bias on the conductor is more negative than the floating potential, the sheath over the conductor side will be thicker. Owing to the potential difference across the material interface, the electric field is no longer perpendicular to the surface. Thus, ion flow near the material interface can be diverted by the multidimensional electric field. The ion flux, ion energy distribution, and ion angular distribution along the surface can be drastically changed, depending on the magnitude of the sheath disturbance.

The situation depicted in Fig. 1 can be encountered in plasma reactors at the interface between a silicon wafer and the substrate holding the wafer. The decollimation of ion trajectories, caused by charging of insulating surfaces, has been studied before.[4–7] In theses studies, however, the electric field distortion was confined to a small region (several μm) near the insulating feature, i.e., the sheath was one dimensional over much of its length except very near the surface feature.

In this article, we report results of a self-consistent fluid simulation of two-dimensional (2D) sheath formation over a flat wall with an insulator/conductor interface (see Fig. 1) exposed to a high density quiescent (no rf plasma potential) Ar plasma. The conductor side of the interface was biased by a negative dc potential, while the insulator was floating. The simulation predicted the profiles of electric potential and ion density, as well as the ion flux distribution along the surface. The extent and magnitude of the distortion of ion flow, caused by surface charging of the insulator, was studied in terms of the flux and impact angle of ions along the surface. The model is described in Sec. II. Simulation results are discussed in Sec. III. Summary and Conclusions are presented in Sec. IV. Only the dc case is examined in this work. The rf case will be reported in the future.

II. MATHEMATICAL MODEL AND SIMULATION PROCEDURES

A. Fluid simulation

The self-consistent, two-dimensional (x,y) fluid model employed in this study was formulated for a plasma with one type of positive ions and electrons. The governing equations

[a)]Author to whom correspondence should be addressed; electronic mail: economou@uh.edu

 © 2003 American Institute of Physics

Downloaded 30 Oct 2003 to 129.7.205.161. Redistribution subject to AIP license or copyright, see http://ojps.aip.org/japo/japcr.jsp

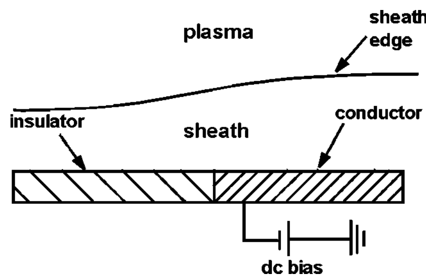

FIG. 1. Schematic (not to scale) of sheath formation over a flat, electrically inhomogeneous surface exposed to plasma. A semi-infinite electrically floating insulator is in contact with a semi-infinite conductor biased by a negative dc voltage. The plasma potential is Φ_p and the conductor bias is Φ_w. The floating potential Φ_f on the surface of the insulator is in general a function of location along the surface.

were the mass and momentum balance equations for ions, coupled with Poisson's equation for the electric potential.[1,8] It was assumed that the ion distribution function was a drifting Maxwellian and the electron distribution function was Maxwellian. The Boltzmann relation was used for the electron density, neglecting electron inertia. Isothermal equations of state were used for both electrons and ions. The background neutral gas pressure and temperature (hence density) were taken to be uniform throughout.

The ion mass and momentum balance equations read

$$\frac{\partial n_i}{\partial t}+\nabla\circ(n_i\vec{u})=0, \tag{1}$$

$$\frac{\partial}{\partial t}(n_i\vec{u})+\nabla\circ(n_i\vec{u}\vec{u})=-\frac{en_i}{m_i}\nabla\Phi-\nu_m n_i\vec{u}, \tag{2}$$

where n_i, m_i, and $\mathbf{u}$ are the ion density, ion mass, and ion fluid velocity, respectively. Φ is the electric potential and e is the elementary charge; ν_m is the total collision frequency for momentum exchange of ions (elastic scattering and charge exchange collisions) with the background gas. The ion pressure force was ignored because the ion thermal energy is much lower than the drift energy (cold ion approximation).

Poisson's equation with the Boltzmann relation for electrons reads

$$\nabla^2\Phi=-\frac{e}{\varepsilon_o}\left(n_i-n_o\exp\left(\frac{\Phi-\Phi_o}{T_e}\right)\right), \tag{3}$$

where ε_o is the permittivity of free space, T_e is the electron temperature (in V), and Φ_o and n_o are the values for electric potential and ion density, respectively, at the top boundary of the domain (see Fig. 2). Since electrons see only a repelling potential, the electron energy distribution function should remain Maxwellian at the same temperature T_e.[9]

The simulation domain and boundary conditions are shown in Fig. 2. The location of the top boundary was far enough from the sheath edge so that a quasineutrality condition could be applied at the top. The domain height (1000 μm) was much larger than the sheath thickness for all cases studied. At the top boundary the plasma density ($n_o=n_i=n_e$) and the electric potential (Φ_o) were specified. The electric potential was assumed to vary only in the vertical direction on both side boundaries ($\partial\Phi/\partial x=0$). The width of the domain was 1000 μm in most cases. This was far enough from the interface for the sheath to be effectively one dimensional at the lateral edges of the domain. A domain width of 1600 μm was used in several cases of thicker sheath to again ensure a one-dimensional sheath at the lateral edges. A flat wall was located at the bottom of the domain. Half of the wall was a perfect conductor with a specified potential, Φ_w. The application of such a bias was assumed not to change the plasma properties (electron density and temperature), i.e., the plasma was sustained independently of the presence of the material wall. The other half of the wall was a perfect insulator. Both conductor and insulator were of semi-infinite extent, i.e., the sheath reached its undisturbed state over the respective material far enough to the left and to the right of the interface. The insulating surface achieved the floating potential, Φ_f, which was a function of position and was found as part of the solution (see below). The plasma sheath evolved self-consistently in accordance with the specified parameters (n_o, T_e, Φ_o, and Φ_w).

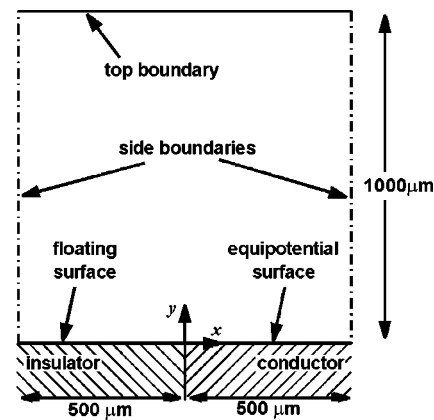

FIG. 2. Simulation domain and boundary conditions. A high density Ar plasma was in contact with a flat, electrically inhomogeneous wall such as shown in Fig. 1. The plasma density n_o and the electric potential Φ_o were specified at the top boundary, which was 1000 μm above the wall. The electric potential at both side boundaries was assumed to vary only in the vertical direction ($\partial\Phi/\partial x=0$). The dc potential on the conductor surface was set at Φ_w. The insulator side of the wall was floating and its surface potential was found as part of the solution.

B. Numerical solution method

Equations (1) and (2) were discretized in space using a multidimensional flux-corrected transport (FCT) scheme developed by Zalesak.[10] In FCT, a weighted average of low order and high order fluxes is used for the convective flux terms in the governing equations. The FCT solutions are stable and also have higher accuracy compared to low order solutions. In this study, second order central difference was used for the high order flux and Rusanov's method, an improvement of Rax's method, was used for the low order flux.[1] Equations (1) and (2) were integrated in time using an Adams–Bashforth second order method. The time step was chosen so that the Courant–Friderichs–Levy condition was satisfied. At the end of each time step, Poisson's equation was solved by a Newton–Raphson method combined with a

Downloaded 30 Oct 2003 to 129.7.205.161. Redistribution subject to AIP license or copyright, see http://ojps.aip.org/japo/japcr.jsp

conjugate gradient scheme to update the electric potential. The simulation evolved until a steady-state solution was reached.

C. Surface charging and floating potential

The conductor surface can draw a net current, but the charge in the conductor rearranges instantaneously so that the conductor remains equipotential (conductivity is infinite).[11] On the other hand, upon exposure to plasma, charge accumulates on the insulator surface, until the floating potential is reached at steady state.[9] However, the floating potential depends on the ion flux (one of the unknowns), this flux being a function of position on the insulator surface. Hence, the potential of the insulator as a function of position was determined as part of the solution using a surface charge balance.

The surface charge density ρ_s at any point on the insulator is

$$\frac{\partial \rho_s}{\partial t} = eJ_i - eJ_e, \tag{4}$$

where J_i and J_e are the flux of positive ions and electrons, respectively, onto the surface. Equation (4) does not include any displacement currents (dc case), and assumes a perfect insulator (no surface conduction of charge).

The thermal flux of inertialess electrons is given by

$$J_e = \frac{1}{4} n_o \exp\left(\frac{\Phi_f - \Phi_o}{T_e}\right) \sqrt{\frac{8T_e}{\pi m_e}}, \tag{5}$$

where m_e is the electron mass.

The steady-state floating potential on the insulator surface is attained when $J_i = J_e$, i.e.,

$$\Phi_f = T_e \ln\left(\frac{4J_i}{n_o}\sqrt{\frac{\pi m_e}{8T_e}}\right) + \Phi_o. \tag{6}$$

The floating potential scales with the electron temperature. For a one-dimensional sheath over an infinite floating wall, both the ion flux and the floating potential are uniform over the entire surface. In the present study, however, the ion flux onto the insulating surface is nonuniform, causing the floating potential to vary along the insulator.

Ion bombardment of a surface can result in the emission of secondary electrons.[8,9] The secondary electron emission coefficient can be quite large for some insulators (~one electron per ion). When secondary electron emission from the insulator surface is considered, the floating potential becomes

$$\Phi_f = T_e \ln\left(\frac{4(1+\gamma_{se})J_i}{n_o}\sqrt{\frac{\pi m_e}{8T_e}}\right) + \Phi_o, \tag{7}$$

where γ_{se} is the secondary electron emission coefficient. Emission of secondary electrons makes the floating potential less negative, and thus decreases the sheath potential over the insulator, $\Phi_o - \Phi_f$.

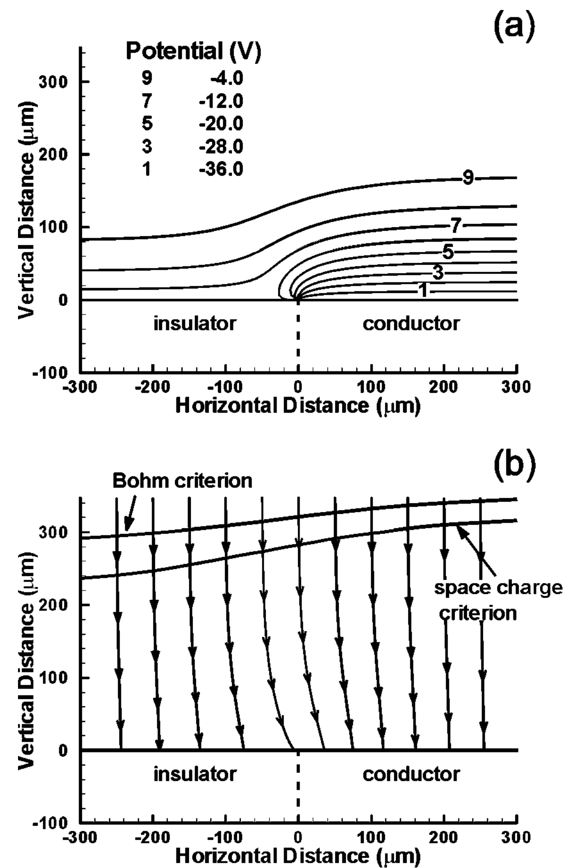

FIG. 3. Electric potential (a) and ion streamlines (b) over the wall, for $n_o = 10^{17}$ m^{-3}, $\Phi_w = -40$ V, $T_e = 3$ eV, and $\gamma_{se} = 0$. The wall potential of the insulator was -14.8 V, far away from the material interface located at $x = 0$. The resulting sheath edge is also shown in (b). The sheath edge by the space charge criterion was defined as the location where the relative net space charge density, $(n_i - n_e)/n_i$, was 0.01. The sheath edge by the Bohm criterion was defined as the locus of points where the ion speed equals the Bohm speed $(u_x^2 + u_y^2)^{1/2} = (kT_e/m_i)^{1/2}$.

III. RESULTS AND DISCUSSION

Figure 3(a) shows the electric potential profile near the insulator/conductor interface, for $n_o = 10^{17}$ m^{-3}, $\Phi_w = -40$ V, $T_e = 3$ eV, and $\gamma_{se} = 0$. The plot covers a horizontal distance of only 600 μm, although the simulation covered a distance of 1000 μm. The potential was referenced with respect to the potential at the top boundary (i.e., $\Phi_o = 0$ V). The background gas pressure was set at 10 mTorr throughout this study. The potential distribution is one dimensional far away from the material interface located at $x = 0$. The sheath potential, a function of horizontal position, is 40 V over the conductor and 14.8 V over the insulator, far away from the interface.[12] The floating potential becomes more negative by ~1.2 V along the insulator surface as the material interface is approached. The sheath potential is larger and the sheath is thicker on the conductor side, compared to the insulator side. The corresponding sheath edge is plotted in Fig. 3(b). The sheath edge was defined as the location where the relative net space charge density $(n_i - n_e)/n_i = 0.01$. The sheath edge gently bends over the interface, becoming horizontal (1D sheath) far away on either side of the interface. The sheath

Downloaded 30 Oct 2003 to 129.7.205.161. Redistribution subject to AIP license or copyright, see http://ojps.aip.org/japo/japcr.jsp

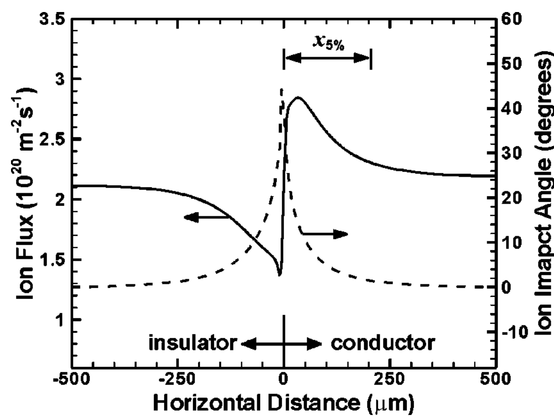

FIG. 4. Ion flux and ion impact angle along the wall for the conditions of Fig. 3. The undisturbed value of the ion flux (calculated far away from the interface, where the sheath was one dimensional) is slightly larger on the conductor side, compared to the insulator side, because of the larger sheath potential. The undisturbed value of the ion flux was 2.19×10^{20} and 2.11×10^{20} m^{-2} s^{-1} for the conductor and insulator surfaces, respectively. The value of $X_{5\%}$, which defines the extent of the ion flow disturbance (see Fig. 8), was 205 μm for this case.

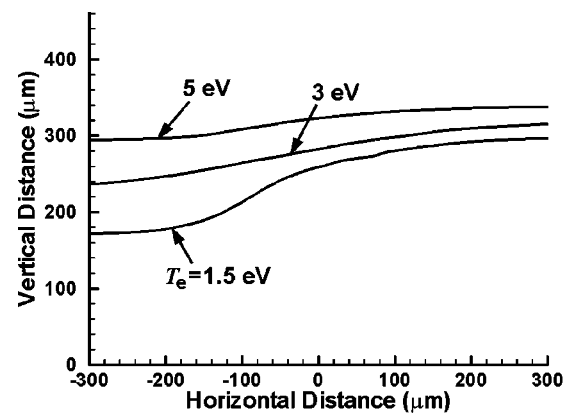

FIG. 5. Contours of sheath edge as a function of the electron temperature for $n_o=10^{17}$ m^{-3}, $\Phi_w=-40$ V, and $\gamma_{se}=0$. The sheath edge was defined as the location where the relative net space charge density was 0.01.

thickness (calculated at a horizontal distance of 500 μm on either side the interface) was 320 and 230 μm over the conductor and the insulator, respectively.

Since the Debye length is much smaller than the ion mean free path in this system, the classic Bohm sheath criterion should be applicable. Figure 3(b) also shows the sheath edge defined as the locus of points where the ion speed equals the Bohm speed. Again, the sheath edge bends gently over the material interface. The sheath defined by the Bohm criterion is thicker than that defined by the space charge criterion, $(n_i-n_e)/n_i=0.01$, since the Bohm "edge" is normally closer to the quasineutral plasma.

Representative ion streamlines are also shown in Fig. 3(b). Outside the sheath edge, the ion streamlines are mainly vertical and equally spaced. This is also the case inside the sheath, at locations far away on either side of the interface. These ions are accelerated by 1D fields. Ions entering the sheath over the material interface, however, are under the influence of a 2D field, which bends the ion trajectories away from the vertical towards the conductor side of the interface. This results in an increase of the ion flux on the conductor at the expense of that on the insulator side of the interface. The ion impact angle is also affected by the 2D fields.

Figure 4 shows the ion flux and ion impact angle along the surface for the same conditions as in Fig. 3. The impact angle was calculated as $\tan^{-1}(-u_x/u_y)$, where u_x and u_y are the horizontal and vertical components of the ion fluid velocity, respectively. As the material interface is approached from the insulator side, the ion impact angle increases drastically, while the ion flux decreases from its undisturbed value. At the interface, the ion impact angle peaks but the ion flux reaches a minimum value. The ion flux increases abruptly as one crosses the interface. Both the ion impact angle and the ion flux decrease gradually to their undisturbed values as one moves further along the conductor surface. The ion impact angle is zero far away on either side of the interface. This implies 1D (along the vertical) ion acceleration. Of course, ion neutral collisions, especially in the pre-sheath, would result in a small angular dispersion of the ion flux, not captured by the fluid simulation. The gross disturbance in ion flux and impact angle near the material interface is caused by the diverging electric field. In addition, the sheath potential varies from 14.8 to 16 V along the insulator surface, and it is 40 V along the conductor surface. Hence, the ion impact energy (not shown), which is equal to the sheath potential in the absence of collisions in the sheath, varies considerably along the surface, especially around the material interface.

The contour shape of the sheath edge over the insulator/conductor wall depends on the electron temperature, as shown in Fig. 5. As the electron temperature is lowered from 5 to 1.5 eV, the sheath thickness shrinks much faster over the insulator side, causing greater disturbance. This is because both the local Debye length and the sheath potential [see Eq. (7)] decrease over the insulator, compared to the conductor, where only the local Debye length decreases but the sheath potential is kept the same. In other words, the difference in sheath thickness over the two sides of the wall is more pronounced at lower electron temperature (see also Table I). As a result, the discontinuous jump of the ion flux across the interface and the maximum ion impact angle both increase as the electron temperature is lowered (see Fig. 6). A similar situation is encountered when the potential of the conductor becomes more negative: the (unperturbed) sheath over the conductor thickens but the sheath thickness over the insulator does not change, exacerbating the distortion of the sheath edge. However, when the plasma density on the top boundary, n_o, was lowered (everything else being the same), the sheath thickness increased by the same factor on both sides of the interface.

When secondary electrons are emitted from the insulating wall, a larger electron influx is needed to balance the surface charge. Secondary electron emission causes the sheath potential and thickness to decrease on the insulator side of the interface, while the sheath thickness remains the same on the conductor side. This makes the sheath thickness difference, and associated disturbance, larger. Figure 7 shows

Downloaded 30 Oct 2003 to 129.7.205.161. Redistribution subject to AIP license or copyright, see http://ojps.aip.org/japo/japcr.jsp

TABLE I. Parameter values used for simulation and resulting sheath thickness. Gas pressure was fixed as 10 mTorr. The surface potential of the conductor Φ_w ranged from -20 to -80 V. The ion density at the top boundary n_o varied from 2×10^{16} to 2×10^{17} m^{-3}. The electron temperature and secondary electron emission coefficient of the insulator were also varied as shown.

Case	n_o (10^{17} m^{-3})	Φ_w (V)	T_e (eV)	γ_{se}	$L_{sh,c}$ [a] (μm)	$L_{sh,d}$ [a] (μm)	$L_{sh,c}-L_{sh,d}$ (μm)
(a)	1.0	−20	3.0	0.0	252	230	22
(b)	1.0	−40	3.0	0.0	320	230	90
(c)	1.0	−60	3.0	0.0	370	230	140
(d)	1.0	−80	3.0	0.0	417	228	189
(e)	1.0	−40	1.5	0.0	296	165	131
(f)	1.0	−40	5.0	0.0	338	292	46
(g)	1.0	−40	5.0	0.5	339	288	51
(h)	1.0	−40	5.0	0.9	336	279	57
(i)	0.2	−20	3.0	0.0	544	506	38
(j)	0.5	−20	3.0	0.0	352	324	28
(k)	2.0	−20	3.0	0.0	181	165	16

[a]The sheath edge was defined as the location where the relative net space charge density was 0.01. The sheath thickness over the conductor ($L_{sh,c}$) and the dielectric insulator ($L_{sh,d}$) was calculated far away from the material interface, where the sheath was one dimensional. The sheath thickness showed a small variation (less than ~1%) for simulation cases using the same plasma parameters, but different mesh resolution.

the ion flux and ion impact angle profiles along the wall for a secondary electron coefficient of the insulator $\gamma_{se}=0.9$. Other conditions were: $n_o=10^{17}$ m^{-3}, $\Phi_w=-40$ V, and $T_e=5$ eV. The case $\gamma_{se}=0$ is also shown for comparison. For $\gamma_{se}=0.9$, the discontinuous jump of ion flux and ion impact angle across the interface are more pronounced. In practice, secondary electrons are accelerated by the sheath field back into the plasma, and can participate in inelastic processes (e.g., ionization) influencing the ionization balance. Such effects were outside the purpose of this study.

Table I summarizes the parameter values used for simulation cases considered in this study, and the resulting sheath thickness. The sheath thickness over the conductor, $L_{sh,c}$, was always larger than that over the dielectric insulator, $L_{sh,d}$. Two new variables were also defined in order to quantify the disturbance of ion flow due to the two-dimensional sheath. These variables were based on the ion flux disturbance on the conductor side. $X_{5\%}$ was defined as the horizontal location, where the ion flux, J, increased by 5% from its undisturbed value, $J_{o,c}$, (i.e., at $x=X_{5\%}$, $J/J_{o,c}=1.05$, see also Fig. 4). $X_{5\%}$ was intended to represent the spatial extent of the disturbance. Furthermore, the magnitude of the disturbance was defined as $(\Delta J_{max}\times X_{5\%})/2$, where $\Delta J_{max}=(J_{max}-J_{o,c})/J_{o,c}$, J_{max} being the maximum value of the ion flux on the conductor side. $(\Delta J_{max}\times X_{5\%})/2$ is roughly proportional to the total current deflected towards the conducting surface. This can be understood by looking at Fig. 4; the ion flux profile on the conductor side from the interface ($x=0$) to $x=X_{5\%}$ is roughly triangular in shape, and the ion current is proportional to the area of the triangle. Figure 8 shows $X_{5\%}$ and $(\Delta J_{max}\times X_{5\%})/2$ as a function of the sheath thickness difference, $\Delta L_{sh}(\equiv L_{sh,c}-L_{sh,d})$, for all cases of Table I. When ΔL_{sh} increases, the sheath edge is more distorted, leading to a greater spatial extent of the ion flow disturbance [Fig. 8(a)], and a larger ion current deflected towards the conductor side of the interface [Fig. 8(b)]. The magnitude of the disturbance is roughly linear with ΔL_{sh} [Fig. 8(b)] for the range of parameter values studied.

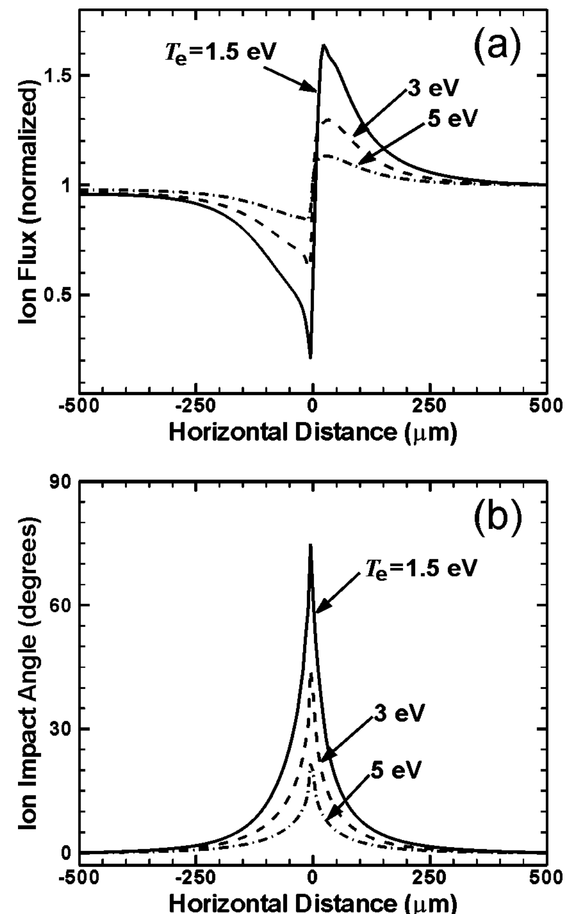

FIG. 6. Ion flux (a) and ion impact angle (b) along the wall as a function of the electron temperature for the conditions of Fig. 5. The ion flux was normalized by its undisturbed value on the conductor side, $J_{o,c}$. $J_{o,c}=1.53\times10^{20}$, 2.19×10^{20}, and 2.85×10^{20} m^{-2} s^{-1} for $T_e=1.5$, 3, and 5 eV, respectively. The undisturbed value of the ion flux on the insulator side $J_{o,d}$, was 1.46×10^{20}, 2.11×10^{20}, and 2.79×10^{20} m^{-2} s^{-1} for $T_e=1.5$, 3, and 5 eV, respectively. The undisturbed value of ion flux was always slightly larger on the conductor side because of the larger sheath potential. When the electron temperature is lowered, the sheath potential over the insulator decreases [see Eq. (7)], but the sheath potential over the conductor remains the same.

Downloaded 30 Oct 2003 to 129.7.205.161. Redistribution subject to AIP license or copyright, see http://ojps.aip.org/japo/japcr.jsp

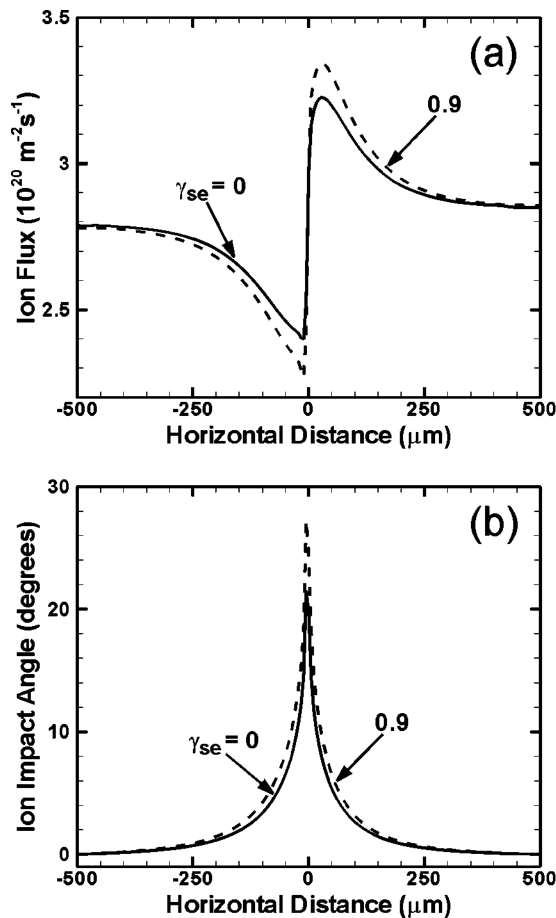

FIG. 7. Ion flux (a) and ion impact angle (b) along the wall as a function of the secondary electron emission coefficient of the insulator surface for $n_o = 10^{17}\ \mathrm{m}^{-3}$, $\Phi_w = -40$ V, and $T_e = 5$ eV.

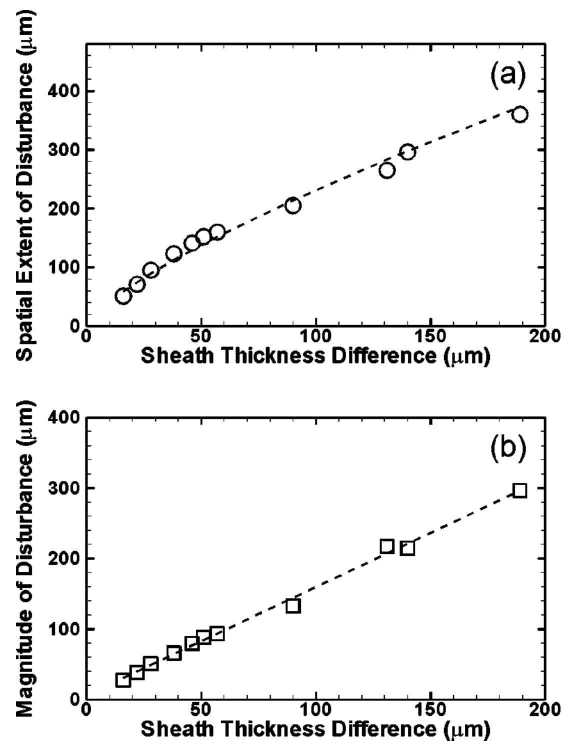

FIG. 8. Spatial extent (a) and magnitude (b) of the ion flow disturbance vs ΔL_{sh} $(\equiv L_{\mathrm{sh},c} - L_{\mathrm{sh},d})$. A least squares fit to the simulation data (symbols) is also shown.

IV. SUMMARY AND CONCLUSIONS

A fluid model and simulation tool were developed to study the structure of the two-dimensional sheath over a flat, electrically inhomogeneous surface, exposed to a high density plasma. The surface was composed of a semi-infinite electrically floating insulator in contact with a semi-infinite conductor biased by a negative dc voltage. Due to surface charge buildup, the sheath potential was smaller over the insulator side, compared to that over the conductor side. This resulted in a 2D sheath structure over the wall. The fluid simulation predicted the 2D electric field, ion density, and ion velocity profiles in the sheath, as well as the ion flux profile along the wall. The 2D electric field decollimated ion trajectories, causing an increase of ion flux on the conductor side of the interface at the expense of the insulator side. As the material interface was approached along the wall from either side, the ion impact angle increased monotonically from normal incidence to a large off-normal angle at the interface. For given plasma density, ion flow disturbance was more pronounced when the electron temperature was lower, or the bias applied to the conductor was more negative, or the secondary electron emission coefficient of the insulator was increased. The spatial extent and magnitude of the ion flux disturbance scaled with the difference in sheath thickness between the two sides of the wall.

ACKNOWLEDGMENTS

Financial support by the National Institute of Standards and Technology, the National Science Foundation (CTS-0072854), and Sandia National Laboratories is greatly appreciated. One of the authors (D. K.) is grateful to Professor F. F. Chen (University of California, Los Angeles) and Professor D. R. Wilton (University of Houston) for helpful discussions. Many thanks go to Dr. G. Hebner of Sandia National Laboratories, Albuquerque, NM, for suggesting this problem to the authors.

[1] D. Kim and D. J. Economou, IEEE Trans. Plasma Sci. **30**, 2048 (2002).
[2] J. R. Woodworth, P. A. Miller, R. J. Shul, I. C. Abraham, B. P. Aragon, T. W. Hamilton, C. G. Willison, D. Kim, and D. J. Economou, J. Vac. Sci. Technol. A **21**, 147 (2003).
[3] D. Kim *et al.*, IEEE Trans. Plasma Sci. (accepted).
[4] D. J. Economou and R. C. Alkire, J. Electrochem. Soc. **135**, 941 (1988).
[5] G. S. Hwang and K. P. Giapis, J. Vac. Sci. Technol. B **15**, 70 (1997).
[6] J. C. Arnold and H. H. Sawin, J. Appl. Phys. **70**, 5314 (1991).
[7] T. Kinoshita, M. Hane, and J. P. McVittie, J. Vac. Sci. Technol. B **14**, 560 (1996).
[8] M. A. Lieberman and A. J. Lichtenberg, *Principles of Plasma Discharges and Materials Processing* (Wiley, New York, 1994).
[9] B. Chapman, *Glow Discharge Processes* (Wiley, New York, 1994).
[10] S. T. Zalesak, J. Comput. Phys. **31**, 335 (1979).
[11] W. H. Hayt, *Engineering Electromagnetics* (McGraw-Hill, New York, 1989).
[12] Strictly speaking, the sheath potential is normally defined as the difference in potential between the edge of the sheath and the wall. However, since the potential gradients outside the sheath are very weak, the sheath potential is approximately equal to the potential difference between the upper boundary of Fig. 2, $\Phi_0 = 0$, and the potential of the wall.

Downloaded 30 Oct 2003 to 129.7.205.161. Redistribution subject to AIP license or copyright, see http://ojps.aip.org/japo/japcr.jsp